JOURNAL OF OPTOELECTRONICS AND ADVANCED MATERIALS Vol. 10, No. 8, August 2008, p. 2134 - 2137

Optical properties of $CaF_2:Eu^{3+}$ nanocrystals embedded in transparent oxyfluoride glass ceramic

S POLOSAN*, C. E. SECU
National Institute of Materials Physics, Bucharest-Magurele 077125, ROMANIA

Transparent oxyfluoride glass ceramic in the system SiO_2–Al_2O_3–CaF_2–EuF_2 containing $CaF_2:Eu^{3+}$ nanocrystals were produced by annealing of the initial glasses slightly above the CaF_2 phase crystallisation peak. The relative good transparency of these materials was due to the small, 65 nm, nucleated CaF_2 nanocrystallites. X-ray diffraction data have shown an increase of the cell parameters for $CaF_2:Eu^{3+}$ compared with CaF_2 which was attributed to the substitution of Ca^{2+} ions with Eu^{3+} ions in the CaF_2 nanoparticles. Optical investigations using UV–VIS-NIR absorption and luminescence spectroscopy have shown an increase of the splitting of the Eu^{3+}-ion associated luminescences and small shifts of the Eu^{3+}-ion characteristic IR absorption peaks. These effects have been attributed to the Eu^{3+} environment evolving from the glass to the crystalline-like one.

(Received February 20, 2008; accepted June 30, 2008)

Keywords: Glass ceramic, CaF_2 nanocrystals, Optical absorption, Luminescence

1. Introduction

Glass ceramics are materials formed through the controlled nucleation and crystallisation of glass, where the amount of residual glassy phase is usually less than 50%. Through a controlled nucleation and crystallisation the precursor glass is thermally converted into a glass-ceramic formed by a nano-crystalline phase dispersed within a glass matrix [1,2].

New transparent oxyfluoride glass-ceramics, in which the optically active ion partitions into a fluoride crystal phase offer an economical alternative with substantial performance improvements over fluoride glasses since they combine the optical advantage of a pure fluoride environment around the rare earth ions, while keeping the thermal and chemical advantages of oxide glasses [3,4]. Great care in fabricating the transparent glass–ceramic has to be taken when choosing the thermal treatment. The annealing (temperature and time) has to be tailored in order to achieve a compromise between the longer times and/or higher temperature, required to have the optimal crystal structure around the active ions and higher luminescence efficiency, while still arranging that the crystals have not grown too large to reduce significantly the transparency of the material.

Among fluorides, the CaF_2 crystal is an important optical material with high solubility of both sensitizer and activator rare earth ions. So far studies have been carried out on the preparation methods, crystallization and optical properties of rare-earth doped CaF_2 nano-crystals embedded in glassy systems [5-9]

In this paper, we have successfully prepared transparent glass ceramics containing Eu^{3+}-doped CaF_2 nano-crystals using the controlled crystallization of melt-quenched glass and we investigated their absorption spectra, emission spectra and luminescence lifetimes.

2. Experimental

2.1 Sample preparation

Glass with the composition of ($50SiO_2$–$30Al_2O_3$-$20CaF_2$-$1EuF_2$) (mol%) were prepared from high purity materials [10]. The constituent chemicals were molten in a corundum crucible at 1300°C in open atmosphere, poured on a platinum plate and cooled bellow the glass temperature of 605°C (resulted from the DSC measurements). The glass was kept at this temperature for about 1h to relinquish the inner stress and then was cooled natural to room temperature. Glass-ceramics have been obtained after subsequently annealed at about 760°C for various times (from 2 to 18 minutes) in open atmosphere. This temperature is slightly above the CaF_2 phase crystallization peak at about 680°C [10]. Annealing at a slightly higher temperature has assured a faster ceramization of the precursor glass and bigger nanocrystals. After the preparation the precursor glass was clear-transparent, but after annealing there was evidence of crystallization in all of the glasses, ranging from a transparent glass to one which was milky white.

2.2 Samples characterization

The samples were characterized by X-ray diffraction (XRD) using a Bruker AXS D8-Advance X- ray powder diffractometer using CuKα incident radiation.

Optical absorption spectra have been recorded in the UV-VIS region 200-1100nm and in the IR region 400-7000 cm^{-1} using commercial Perkin-Elmer spectrophotometers.
Photoluminescence (PL) spectra have been recorded using lock-in technique with a standard luminescence home-made set-up composed of two monochromators for excitation and emission, a Xe-150W lamp as light source and a photomultiplier as light detector. For the luminescence lifetimes measurements a box-car integrator has been used.

3. Results and discussions

The X-ray diffraction (XRD) pattern of the precursor glass has shown that the glass is completely amorphous without crystallization peaks. However, after annealing we have easily recognized extra-diffraction peaks ascribed to the CaF_2 crystalline phase precipitation in the glass matrix (Fig. 1). As can be seen the line positions agree with those predicted for the cubic CaF_2 (open dots in the Fig. 1 - reference # 01-075-0097 in the JCPDS database). The small peak at 31.82°, which marks the [200] XRD line, is characteristic for the substitutions of Ca^{2+} ions by the Eu^{3+} ions [5]. In the XRD pattern we have also observed a small peak at 26.6° which was associated with the [111] XRD line characteristic for the substitution of Ca^{2+} ions by the Eu^{2+} ions (closed triangles in the Fig. 1).

As can be observed the Eu^{2+} ions have been oxidized to Eu^{3+} ions due to the oxidizing atmosphere in which the annealing was performed. From the analysis of the *d* values of the XRD peaks we have observed an increase of the lattice constant from 5.457 Å to 5.497 Å which is consistent with the Eu^{3+}-ion incorporation inside the CaF_2 nanocrystals [11, 12].

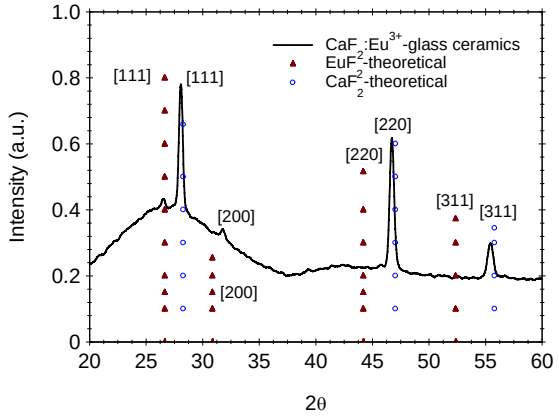

Fig. 1. The X-Ray diffraction pattern of precursor glass (a) and oxyfluoride glass-ceramic annealed at 760°C for 15 min. (b).

The mean size of the nanocrystals was calculated from the XRD pattern (Figure 1) using Debye-Scherrer equations:

$$B * \cos\theta = \frac{K\lambda}{D} + \eta * \sin\theta$$

where θ is the angle of the XRD peak, λ is the X-ray wavelength (1.54056 Å), B is the width of the XRD peak at half height and K is a shape factor (which is about 0.94 for cubic nanoparticles) and η is the strain in the crystallites. There are many parameters which determine the width B of a diffraction peak, but the main one is the instrumental factor, i.e. the correction of the B factor that can be found by using a standard diffraction powder with a known size. By plotting "B·cosθ" vs. "sinθ" we will get a straight line with slope η that intercept the Oy axis at and $K\lambda/D$. In order to calculate the size of nanocrystals we have used the Debye-Scherrer equation and the first five peaks of CaF_2 observed in the XRD pattern (Figure 2) recorded by us up to 80° angle (but not shown in the Fig. 1).

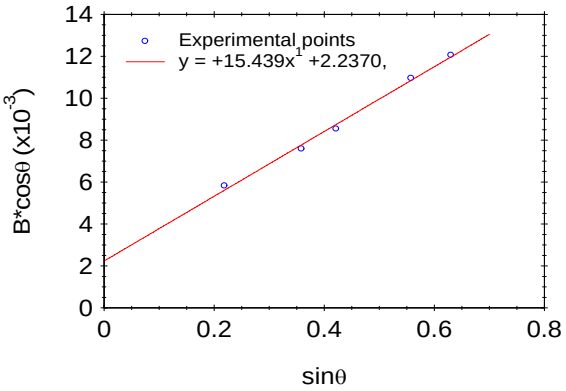

Fig. 2. The dependence of the "B.cosθ" vs. "sinθ" used for the calculation of the nanoparticles size.

The intercept of the Oy axis is at $2.237 \cdot 10^{-3}$ which yield about 65nm for the size of the CaF_2 nanocrystals. The level of the crystallization has been computed by comparing the areas under the XRD peaks of CaF_2 nanoparticles with the total area under the XRD curve which yielded about 3-4% nano-crystalline phase dispersed within a glass matrix. The crystallization is quite at low level compared with similar glass-ceramics [1,2] but enough to change the transmission of the glass-ceramics.

In the optical absorption spectra recorded in the UV-VIS region (Fig. 2) we have observed the glass absorption edge at about 320nm on which are superimposed two small peaks at about 392nm and 415nm due to the $^5F_0 \rightarrow {}^5L_6$ and $^5F_1 \rightarrow {}^5D_3$ transitions of the Eu^{3+} ions present in the initial glass [13].

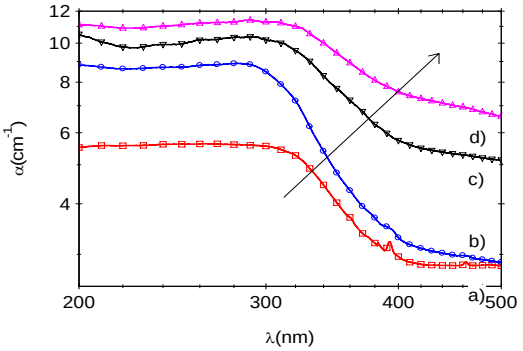

Fig. 2. Optical absorption spectra of Eu^{3+}-doped oxy-fluoride glasses (shown in logarithmic scale): precursor glass (a) and glass-ceramics annealed in air at 760 °C for 2 min. (b), 8 min. (c) and 15 min. (d). The arrow indicates increasing annealing time.

A transparency region can be observed at longer wavelengths where the extinction coefficient falls with a k^n wavelength dependence, with n≈4–5. This suggests that Rayleigh scattering is the dominant mechanism in this region [14]. The effect of particle growth during annealing can be clearly seen by the displacement of the scattering spectrum to longer wavelengths with increasing annealing times [14]. The relative good transparency of glass ceramic was ascribed to weak light scattering as a result of the smallness of the nanocrystals with respect to the wavelength of visible light and provides a prerequisite condition for applications.

In the infrared absorption spectra (FTIR) we have observed several peaks at 3490nm ($^7F_0 \rightarrow {}^7F_4$), 2638nm ($^7F_1 \rightarrow {}^7F_5$) and 2068nm ($^5F_0 \rightarrow {}^7F_6$) which are due to the Eu^{3+}-ion transitions [12]. With the increase the annealing time the $^7F_0 \rightarrow {}^7F_4$ and $^7F_0 \rightarrow {}^7F_6$ peaks slightly shift to higher energies with about $40cm^{-1}$ and $10cm^{-1}$, respectively. This effect that was tentatively associated with a change of the Eu^{3+}-ion environment from glass to nanocrystals.

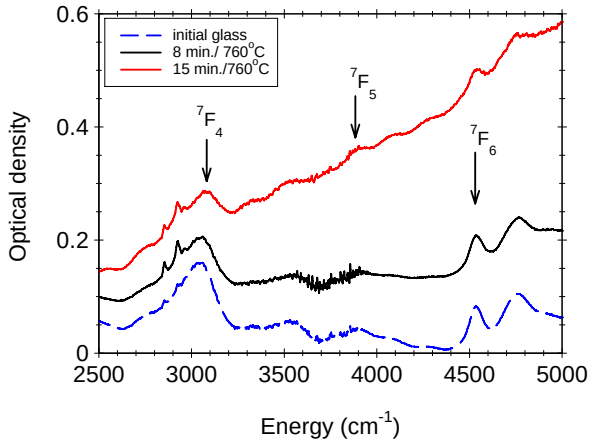

Fig. 3. Infrared absorption spectra (FTIR) of Eu^{3+}-doped oxy-fluoride glasses: precursor glass (a) and glass-ceramics annealed in air at 760°C for 2 min. (b), 8 min. (c) and 15 min. (d).

In the photoluminescence spectra excited at 390nm (in the Eu^{3+}-ion absorption band [12]) we have observed the Eu^{3+}-ion luminescences associated with the ($^5D_0 \rightarrow {}^7F_J$ and ($^5D_1 \rightarrow {}^7F_J$) radiative transitions [12]. In the initial glass sample, Eu^{3+} ions are randomly dispersed among the oxyfluoride glassy matrix, and the luminescence bands exhibit the Stark splitting with several weak components. In the glass ceramic the splitting is better resolved (in the 575-610nm region) which indicated that the Eu^{3+} ions had been incorporated into the CaF_2 crystalline environment [7, 15]. We have not observed the Eu^{2+}-ion luminescence [8] because they have been reduced almost completely to the Eu^{3+} ions and its luminescence is very week being covered by the intrinsic glass luminescence [8].

A clear increase of the luminescence (with a factor of about two) has been observed in the glass-ceramic compared to the initial glass (Fig. 4). In the oxide glasses the rare-earth ion do not emit efficiently since the highest vibrational frequency of the surrounding (ν_{max}) of the ion is about 1000-1200cm^{-1} and therefore the rate of the non-radiative transitions is quite high [14]. The situation changes in fluorides where ν_{max} is smaller and therefore the contribution of the non-radiative transitions decreases, i.e. the luminescence efficiency is higher as we have observed (Fig. 4).

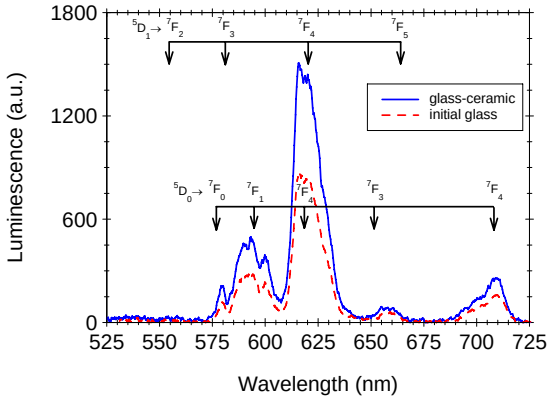

Fig. 4. The photoluminescence spectra recorded on initial glass and glass-ceramic annealed at 760°C for 15 min. ($\lambda_{ex.}$=392nm).

As can be seen in the Fig.4 the intensities of the $^5D_0 \rightarrow {}^7F_1$ and $^5D_0 \rightarrow {}^7F_2$ transitions are comparable which indicated that the Eu^{3+} are rather localized in non-centrosymmetric sites of the CaF_2 nanocrystals structure [13,16]. This observation is in good agreement with previous studies where it was shown that the substitution of Ca^{2+} ions by trivalent rare earth cations leads to several different symmetries for the rare earth sites, with some of them non-centrosymmetric [17]. In the case of Eu^{3+} the ions are entering in CaF_2 crystal in C_{4v} sites symmetries [18].

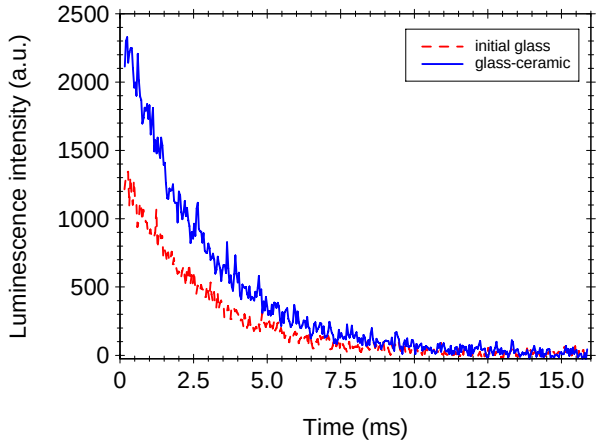

Fig.5. Luminescence decay curves recorded at 620nm on initial glass and glass-ceramic annealed at 760°C for 15 min ($\lambda_{ex.}$=392nm).

The luminescence decay curve of the $^5D_0$ state was obtained by monitoring the 620nm ($^5D_0 \rightarrow {}^7F_2$) emission of Eu^{3+} ion (Fig. 5). The luminescence decay curves were approximately fitted with single exponentials having the characteristic times of 2.75±0.02ms in initial glass and 2.65±0.02ms in the glass ceramic. The characteristic lifetimes agree with similar data reported in powdered $CaF_2:Eu^{3+}$ (10%) where a value of about 3ms was found for the lifetime [19].

4. Conclusions

A transparent oxy-fluoride glass ceramics containing Eu^{3+}-doped CaF_2 nano-crystals has been made using the controlled crystallization of melt-quenched glass The relative good transparency of these materials was due to the small size (about 65nm), nucleated CaF_2 nanocrystallites. X-ray diffraction data have shown that active Eu^{3+} rare earth ions are embedded into the low phonon energy CaF_2 nanocrystals. Optical absorption and luminescence spectroscopy have shown how the Eu^{3+} environment evolves from the glass to the crystalline-like one. Glass ceramization results in about 50% improvement in luminescence associated with Eu^{3+} ion.

Acknowledgements

The financial support of the Romanian Research Ministry, PN II Research grant No. 71-007 / 2007 is gratefully acknowledged.

References

[1] M. Mortier, Phylosofical Magazine B **82**(6), 745 (2002).
[2] M. Clara Gonçalves, Luís F. Santos, Rui M. Almeida, C. R. Chimie **5**, 845 (2002).
[3] M.J. Dejneka, J. Non-Cryst. Solids **239**, 149 (1998).
[4] Y. Wang, J. Ohwaki, Appl. Phys. Lett. **63**, 3268 (1993).
[5] J. Labéqueria, P. Gredin, M. Mortier, G. Patriarche, A. De Kozak, Z. Anorg. Allg. Chem. **632**, 1538 (2006)
[6] A. Bensalah, M. Mortier, G. Patriarche, P. Gredin, D. Vivien Journal of Solid State Chemistry **179**, 2636 (2006).
[7] Zhongjian Hu, Yuansheng Wang, En Ma, Feng Bao, Yunlong Yu, Daqin Chen Materials Research Bulletin **41**, 217 (2006).
[8] J. Fu, J.M. Parker, P.S. Flower, R.M. Brown, Mater. Res. Bull. **37**, 1843 (2002).
[9] G. A. Kumar, C. W. Chen, R. Riman, S. Chen, D. Smith, J. Ballato Applied Physics Letters **86**, 241105 (2005)
[10] X.Qiao, X. Fan, M.Wang,Jean-Luc Adam, X.Zhang, J.Phys.:Condens. Matter **18**, 6937 (2006).
[11] F. Wang, X. Fan, D. Pi and M Wang, Solid State Communications **133**, 775 (2005).
[12] Yuki Kishi and Setsuhisa Tanabe,Shigemi Tochino, Giuseppe Pezzotti, J. Am. Ceram. Soc., **88**(12) 3423 (2005).
[13] M.J. Dejneka, E.Snitzer, R.E. Riman, J. Luminescence **65**, 227 (1995)
[14] A. Edgar, G. V. M. Williams, J. Hamlin, M. Secu, S. Schweizer, J.-M. Spaeth, Current Applied Physics **4**(2-4), 193 (2004).
[15] Xvsheng Qiao, Xianping Fan, Jin Wang, Minquan Wang, Journal of Non-Crystalline Solids **351**, 357 (2005).
[16] G. Blasse and B.C.Grabmaier Luminescent Materials, Springer Verlag (1994).
[17] P. Dorenbos, H.W. den Hartog, Phys. Rev. B **31**, 3932 (1985).
[18] S. Robinet, D. Trottier, J. Tendil, J. C. Cousseins, Eur.J. Solid State Inorg. Chem. **32**, 169 (1995).
[19] S. Robinet, D.Trottier, J.Tendil, J. C.Cousseins, Eur. J. Solid State Inorg. Chem. **31**, 1 (1994).

*Corresponding author: silv@infim.ro